Defluoridation by magnesia-pullulan: surface complexation modeling and pH neutralization of treated fluoride water by aluminum

Yuanyao Ye[a,b], Wenbo Liu[c], Wei Jiang[a*], Jianxiong Kang[a], Huu Hao Ngo[b], Wenshan Guo[b], Yiwen Liu[b]

[a]*School of Environmental Science and Engineering, Huazhong University of Science and Technology, No. 1037 Luoyu Road, Wuhan 430074, PR China*
[b]*Centre for Technology in Water and Wastewater, School of Civil and Environmental Engineering, University of Technology Sydney, Sydney, NSW 2007, Australia*
[c]*Wuhan Urban Construction Investment & Development Group Co., Ltd. , PR China.*

**Corresponding author. Tel: +86 02787792512.*

E-mail address: jiangwei0707@hust.edu.cn & jxkang@hust.edu.cn

Abstract

The magnesia-pullulan composite (MgOP) achieved effective fluoride removal in previous research. In the present study, an acid-base titration experiment was conducted to investigate the properties of MgOP surface and further explore the mechanism of fluoride adsorption on MgOP. Results showed that the presence of chloride ions could improve fluoride adsorption on MgOP; however, additional nitrate ions had negligible impacts. A diffuse layer model and chemical equilibrium software (Visual MINTEQ 3.1) were used to simulate the acid-base titration data. The effects of initial pH values on the rate of fluoride uptake by MgOP were also studied. Moreover, aluminum salts were added to the fluoride solution with MgOP for the pH neutralization of treated water, in which aluminum chloride was preferred.

Keywords: magnesia-pullulan composite, defluoridation, adsorption, surface complexation, pH neutralization

1. Introduction

Trace amounts of fluoride (0.4–0.6 mg/L) in drinking water are beneficial for human health [1]. However, long-duration exposure to drinking water containing more than 1.5 fluoride mg/L may result in diseases such as skeletal fluorosis and cancer [2]. Notably, the disorder caused by fluorosis is not reversible and has no medical treatment [3]. The World Health Organization (WHO) has determined that the fluoride concentration in drinking water should be maintained below 1.5 mg/L [4]. Nevertheless, there are still over 200 million people who are exposed to drinking water contaminated by fluoride [5, 6]. For this reason, an efficient and effective technique for fluoride removal is urgently needed.

Compared to other methods (e.g., precipitation-coagulation process and membrane hybrid system), adsorption for fluoride removal from water has attracted considerable attention due to its low cost, high stability, and simple operation and design [7, 8]. Magnesia (MgO) has been widely investigated as an adsorbent to remove fluoride because: (1) it presents high defluoridation capacity; (2) its cost is low; and (3) the high pH_{zpc} of MgO (12.1-12.7) can enhance the fluoride adsorption because of electrostatic attraction when the pH value of solution is lower than that of the isoelectric point [9, 10]. However, several drawbacks may negatively affect its application for the fluoride removal such as minimum, equilibrated time of 60 min [11]. More importantly, to support the transfer of inert water through the small passages and interstices between the MgO particles, greater back pressure is needed for fine porosity necessitates [11]. Therefore, recent efforts have been directed towards MgO modification to address the disadvantages [9, 12-14]. From the previous study [15], a new adsorbent was developed by calcining pullulan and MgO, in which pullulan (a biocomposite) can increase the accessibility of the adsorbate-binding sites due to abundant hydroxyl groups existing in its saccharide unit. Results derived from the batch experiment of fluoride adsorption confirmed that the magnesia-pullulan composite (MgOP) (i.e. adsorbent)

had higher adsorption capacity of fluoride and shorter equilibrium time when compared to the other similar adsorbents [13, 16, 17]. Moreover, even though many modified MgO adsorbents have high adsorption capacity for fluoride ions, the adsorption performance is seriously influenced by increasing pH [12-14, 16-18]. By contrast, effective fluoride removal through MgOP can be achieved over a wide pH range (3-12). This can increase the practical application prospects of MgOP for the fluoride removal. Besides, the regenerate efficiency of fluoride-loaded MgOP can be up to 99% [19], which is much higher than that of the similar, modified MgO adsorbents [9, 13, 14]. The preparation process of MgOP is also simpler when compared to other similar adsorbents [13]. However, the pH of treated fluoride solution increased to >10.0, probably due to the presence of oxide in the MgOP, which is consistent with other modified MgO adsorbents [9, 14]. This may negatively affect the fluoride adsorption by MgOP because the additional acid solution may be needed for the pH neutralization of treated water.

For this reason, to neutralize the pH of treated water, aluminum salts were preferred as an assistant substance to be added into the fluoride solution along with MgOP since: (i) they have amphoteric property, which can effectively buffer pH of treated fluoride solution; and (ii) their modified forms could also remove fluoride from water [20], which indicates that the addition of aluminum salts may have insignificant impacts on the defluoridation efficiency of MgOP. It should be noted here that the reaction between fluoride and aluminum in water may follow the pathway: firstly, fluoride is adsorbed by aluminum hydroxide ($Al[OH]_3$) followed by formation of Al-F-OH precipitates [21]. Moreover, the effects of pH on the adsorption rate of fluoride ions were explored. In this paper, another main objective is to investigate the acid-base surface properties of MgOP to determine the pH effects on fluoride adsorption. This would be important when, for example, the pH of fluoride solution to be treated was elevated. Surface complexation models (SCMs) are typically used to explore the interaction between

the solutes and functional groups on the surface of an adsorbent, as well as how pH affects the adsorption process [20, 22, 23]. In the present study, a diffuse layer model (DLM) as the SCM was utilized to simulate the acid-base titration data with the help of the chemical equilibrium software Visual MINTEQ 3.1 (https://vminteq.lwr.kth.se/). The DLM needs fewer simulation parameters than other similar models [24], resulting in simpler calculation process and more accurate results.

2. Experimental Section

2.1. Preparation of MgOP

According to the previous study [19], 8 g of MgO (Sinopharm Chemical Reagent Co., Ltd, Shanghai, China) and 12 g of pullulan (Shandong Freda Biotechnology Co., Ltd, Linxi, China) were firstly added into a 1000-mL polypropylene beaker in the weight ratio of 2:3, along with 400 mL of deionized water (ddH_2O). The mixture was stirred for 24 h at room temperature and then dried in a drying oven at 105 °C for 12 h. Subsequently, the compound was calcined in a muffle furnace at 450 °C for 2 h. The resulting material (i.e., MgOP) was ground into powder and sieved to obtain 0.074-mm diameter particles. The prepared MgOP was sealed in a hermetic plastic bag for later use.

2.2. Acid-base titrations

The acid-base surface characteristics of MgOP were conducted in a 1000-mL polypropylene beaker at room temperature. First, 2 g of MgOP was soaked in 1000 mL of CO_2-free ddH_2O for 24 h to fully hydrate MgOP and produce a MgOP suspension. Then, a background electrolyte was added to the MgOP suspension at different concentrations (0.001, 0.05, and 0.1 mol/L). A 2 mol/L of acid solution was added to adjust the pH of the MgOP suspension. As a result of this, the pH of MgOP suspension could be quickly decreased with insignificant changes in the total volume of MgOP suspension. However, the pH of the MgOP suspension should be strictly controlled above 2 to avoid the possible dissolution of MgOP. It

should be noted here that the pH value of arbitrary starting point should be much smaller than the zero point of charge (pH_{zpc} = 10.7) [15]. Furthermore, the pH value of MgOP suspension was moderately increased by adding 0.1 mol/L sodium hydroxide (NaOH) solution. Each step was considered stability when the pH variation was less than 0.005/min.

In the titration process, the beaker containing the MgOP suspension was placed on a magnetic stir plate (XK78-1, Jianyan Xinkang Medical Instrument Co., Ltd., Jianyan, China), and a pH probe (pHS-3C, Shanghai REX Instrument Factory Co., Ltd., Shanghai, China) was inserted into the suspension to monitor the pH changes. Moreover, nitrogen gas was continuously supplied in the MgOP suspension to prevent absorption of atmospheric carbon dioxide. In this acid-base titration study, sodium nitrate ($NaNO_3$) and sodium chloride (NaCl) solutions were used as the background electrolytes because the effects of nitrate and chloride ions on the fluoride adsorption by MgOP were smaller when compared to other coexisting anions [15, 19]. Besides, the corresponding acid solutions for adjusting pH were nitric acid (HNO_3) and hydrochloric acid (HCl). The titration data obtained without fluoride ions were utilized by DLM to calculate the intrinsic acidity constants of MgOP. All titration experiments also were conducted in the absence of MgOP to obtain the "blank" data for comparison.

2.3. Adsorption experiments

A standard stock solution of fluoride ions (1000 mg/L) was prepared by dissolving sodium fluoride (NaF) in the ddH_2O. Working fluoride solutions were achieved by diluting the standard stock solution. The pH of the fluoride solutions was adjusted by adding 0.1 mol/L of NaOH and HCl solutions. The effects of aluminum salts on fluoride adsorption were examined using 50-mL polypropylene tubes that contained aluminum salts, MgOP and fluoride solutions. In the experiment, the tube was shaken in a thermostatic shaker at 150 rpm and 25 °C, after which the mixture was centrifuged at 3000 rpm for 20 min. Then the

supernatant was filtered through a 0.45-μm membrane filter (Tianjin Jinteng Experimental Equipment Co. Ltd., Tianjin, China) for the later measurement. The resulting fluoride concentrations were determined using an ion meter and ion selective electrodes (Shanghai branch pXS-215, Tianda Instrument Shanghai, Co., Ltd., Shanghai, China). The pH was measured using the pH meter. The concentration of Al^{3+} ions was monitored by the spectrometric method using pyrocatechol violet (Shanghai INESA Scientific Instrument Co., Ltd., Shanghai, China).

The adsorption isotherms, kinetics and thermodynamics also were investigated to determine fluoride adsorption by MgOP in the presence of Al^{3+} ions. All experiments were repeated three times at least under identical conditions with using the data's standard deviations. The defluoridation capacity of MgOP was calculated using Equation (1) [25]:

$$q_t = \frac{(C_0 - C_t) \times V}{W} \quad (1)$$

where q_t (mg/g) is the defluoridation capacity of MgOP at time t (min); C_0 and C_t (mg/L) are the initial and remaining concentrations of fluoride ions at time t, respectively; V (L) is the volume of fluoride solution; and W (g) is the dry weight of MgOP.

3. Results and discussion

3.1. Acid-base surface chemistry of MgOP

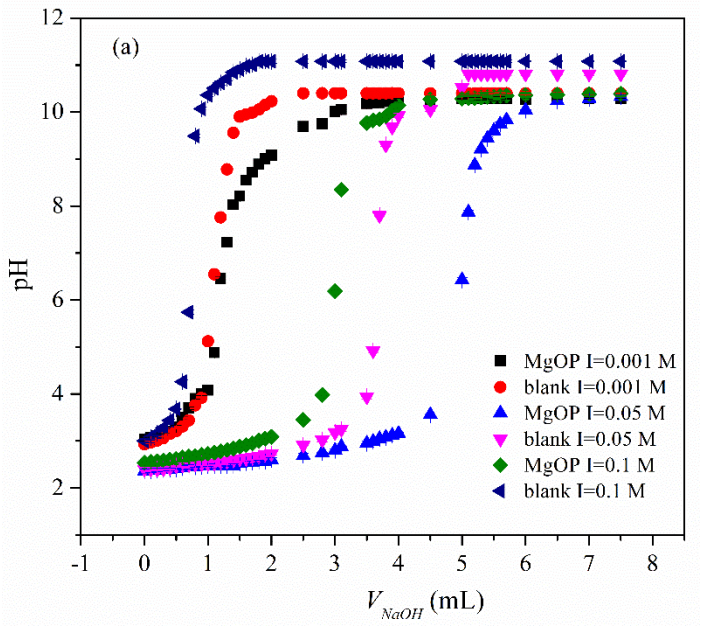

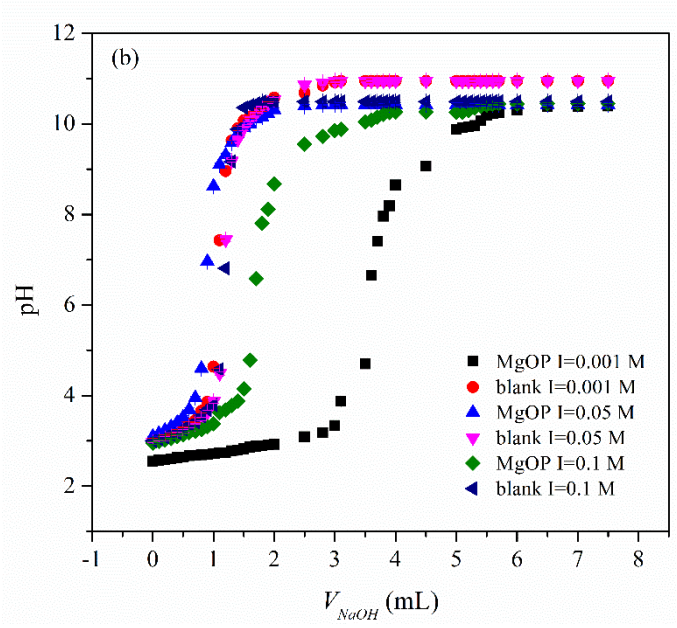

Fig. 1. The surface acid-base titration plots for MgOP with (a) NaCl and (b) $NaNO_3$ as the background electrolyte (C_{MgOP} = 2 g/L, temperature = 25 °C, "I" represents the ionic strength of the solution, and "blank" reflects the surface acid-base titration experiment conducted without MgOP).

From Fig. 1, the added OH^- ions were involved in three reactions during the titration process: pH neutralization of the MgOP suspension; reactions with the functional groups on the MgOP surface; and pH elevation of the MgOP suspension. In contrast, the added OH^- ions were only involved in the pH neutralization in the absence of MgOP (i.e., the blank experiment). Besides, MgOP showed better buffering capacity for pH with increasing concentrations of Cl^- because Cl^- ions could facilitate the surface complexation of MgOP. Consequently, the added OH^- ions may prefer to react with functional groups on the MgOP surface rather than to neutralize pH. By contrary, the surface reactions of MgOP were negatively affected by NO_3^- and most added OH^- ions were thereby involved in pH neutralization. In this scenario, an increased concentration of NO_3^- may weaken the surface reactions of MgOP.

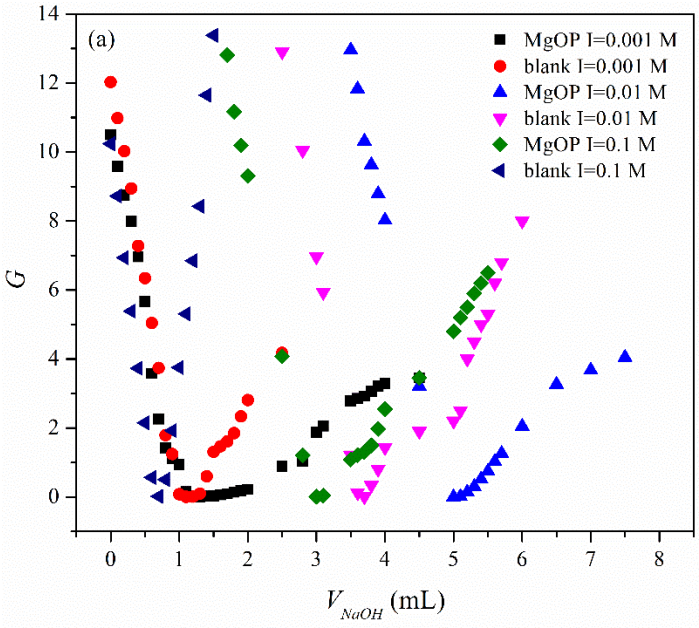

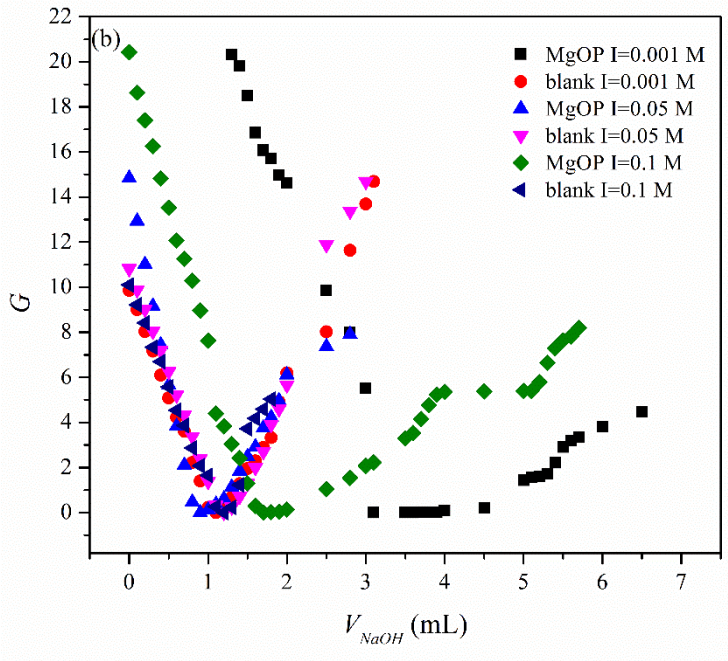

Fig. 2. Gran plots of MgOP with (a) NaCl and (b) $NaNO_3$ as the background electrolyte (C_{MgOP} = 2 g/L, temperature = 25 °C, "I" represents the ionic strength of the solution, "blank" reflects the surface acid-base titration experiment conducted without MgOP, and "G" represents the values of the Gran function).

In this study, Gran plots were used to analyze the MgOP titration data (Fig. 2) and the Gran function (G) was determined by Equations (2) and (3) [26, 27]:

on the acidic side (pH < 7): $G_a = (V_0 + V_{at} + V_b) \times 10^{-pH} \times 100$ (2)

on the alkaline side (pH > 7): $G_b = (V_0 + V_{at} + V_b) \times 10^{pH-13.8} \times 100$ (3)

where V_0 (mL) is the initial volume of the solid suspension; and V_{at} and V_b (mL) are the total volumes of the added acid and alkaline solutions, respectively. Linear regression analysis of the Gran plots yielded values for V_{eb1} and V_{eb2}, which are the intersections of the regressions of the Gran plots with the X-axis. The values of V_{eb1} and V_{eb2} indicated different reactions that added OH^- involved in the MgOP suspension: (a) pH neutralization ($V_{NaOH} < V_{eb1}$); (b) reactions with functional groups on the MgOP surface ($V_{eb1} < V_{NaOH} < V_{eb2}$); and (c) pH elevation ($V_{NaOH} > V_{eb2}$). Thus, V_{eb1} could be considered as the zero point of titration [28], before which most OH^- ions were involved for the pH neutralization instead of the surface reactions of MgOP.

The total concentration of protons consumed in the titration process (*TOTH*) was calculated using Equation (4):

$$TOTH = \frac{-(V_b - V_{eb1}) \times C_b}{V_0 + V_b} \text{ (mol/L)} \quad (4)$$

where C_b (mol/L) is the concentration of NaOH solution. Besides, the density of active surface sites (D_s) (sites/nm^2) and concentrations of surface active sites (H_s) (mmol/L) can be deduced from the Gran plots using Equations (5) and (6):

$$H_s = \frac{(V_{eb2} - V_{eb1})_{sample} \times C_b - (V_{eb2} - V_{eb1})_{blank} \times C_b}{V_0} \quad (5)$$

$$D_s = \frac{H_S \times N_A}{S \times C_S \times 10^8} \quad (6)$$

where $(V_{eb2} - V_{eb1})_{sample}$ and $(V_{eb2} - V_{eb1})_{blank}$ represent sampled and blank data, respectively; S (m^2/g) and C_s (g/L) are the specific surface area and concentration of MgOP, respectively; and N_A (mol^{-1}) is Avogadro's constant (6.022×10^{23}).

Table 1

Titrated parameters and site concentrations of MgOP

Background electrolyte	Ionic Strength (mol/L)		V_{eb1} (mL)	V_{eb2} (mL)	V_{eb2}-V_{eb1} (mL)	D_s (sites/nm^2)	H_s (mmol/L)
NaCl	0.001	sample[a]	1.027	1.745	0.718	4.68	0.511
		blank[b]	0.987	1.194	0.207		
	0.05	sample[a]	4.798	5.224	0.426	2.14	0.234
		blank[b]	3.661	3.853	0.192		
	0.1	sample[a]	2.790	3.140	0.350	1.86	0.203
		blank[b]	0.659	0.806	0.147		
$NaNO_3$	0.001	sample[a]	3.487	4.050	0.563	1.64	0.179
		blank[b]	0.817	1.201	0.384		
	0.05	sample[a]	0.807	1.140	0.533	1.62	0.177
		blank[b]	1.109	1.265	0.356		
	0.1	sample[a]	1.592	2.151	0.559	1.61	0.176
		blank[b]	1.146	1.529	0.383		

[a] "sample" indicates the surface acid-base titration experiment conducted with MgOP.

[b] "blank" indicates the surface acid-base titration experiment conducted without MgOP.

From Table 1, the values of V_{eb1} with $NaNO_3$ as the background electrolyte were greater than those with NaCl as the background electrolyte, which indicated that more added OH^- ions were involved in the pH neutralization of MgOP suspension in the presence of $NaNO_3$. Moreover, the values of $(V_{eb1}\text{-}V_{eb2})_{sample}$ were higher than those of $(V_{eb1} - V_{eb2})_{blank}$ with either NaCl or $NaNO_3$ as the background electrolyte. This confirmed both the occurrence of MgOP's surface complexations and its buffering capacity for pH. More importantly, D_s and H_s were larger with NaCl as the background electrolyte than those with $NaNO_3$ as the background electrolyte. This is because the presence of Cl^- ions could increase the number of active adsorption sites on the surface of MgOP. However, increasing concentrations of Cl^- may also inhibit the generation of active adsorption sites and thereby decrease the values of

231 D_s and H_s. In contrast, there were negligible changes in the D_s and H_s at different
232 concentrations of $NaNO_3$ since NO_3^- ions had insignificant effects on the number of active
233 adsorption sites on the MgOP surface. To sum up, low concentrations of Cl^- could promote
234 the formation of active sites on the MgOP surface and thereby improve the fluoride
235 adsorption while the presence of NO_3^- insignificantly influenced the fluoride adsorption on
236 MgOP. These results also agreed with findings in the previous study [15].
237 The following hypothesis was made for the modeling purposes: (i) most adsorption sites
238 of MgOP are hydroxyl groups; (ii) there are no interactions between two different adsorption
239 sites on the MgOP surface; and (iii) one adsorption site can only bind with one cation [29,
240 30]. The MgOP could be activated to form the surface active hydroxyl groups (≡*SOH*) and
241 the protonation and deprotonation reactions may thus occur in the acid and alkaline
242 environments as indicated by Equations (7) and (8), respectively [28]:
243 protonation: $\equiv SOH + H^+_{(s)} \leftrightarrow \equiv SOH_2^+$ (7)
244 deprotonation: $\equiv SOH \leftrightarrow \equiv SO^- + H^+_{(s)}$ (8)
245 where ≡*SOH*, ≡SOH_2^+ and ≡SO^- represent neutral, positively charged, and negatively
246 charged hydroxyl groups on the MgOP surface, respectively; and $H^+_{(s)}$ is the concentration of
247 H^+ ions on the surface of MgOP. The equilibrium constants of the protonation and
248 deprotonation were calculated by Equations (9) and (10):
249 $$pK_{a1} = \log \frac{\{\equiv SOH_2^+\}}{\{\equiv SOH\}\{H^+\}_s} \quad (9)$$
250 $$pK_{a2} = \log \frac{\{\equiv SO^-\}\{H^+\}_s}{\{\equiv SOH\}} \quad (10)$$
251 where pK_{a1} and pK_{a2} are the equilibrium constants of protonation and deprotonation,
252 respectively; $\{H^+\}_s$ is the proton activity on the MgOP surface; $\{\equiv SOH\}$, $\{\equiv SOH_2^+\}$ and
253 $\{\equiv SO^-\}$ represent activities of original, protonated and deprotonated hydroxyl groups on the

MgOP surface, respectively.

Table 2

Surface intrinsic constants of MgOP

Background electrolyte	NaCl			$NaNO_3$		
Ionic strength (mol/L)	0.001	0.05	0.1	0.001	0.05	0.1
pK_1	6.387	6.477	6.749	6.935	6.849	6.994
pK_2	-6.388	-6.388	-6.068	-6.048	-6.348	-5.938

According to the DLM, the equilibrium constants of protonation and deprotonation of MgOP were calculated using Visual MINTEQ 3.1 software (Table 2). The values of pK_{a1} were greater than those of pK_{a2} at all ionic strengths of the two background electrolytes, which meant it was more easily for MgOP to bind with H^+ than OH^- ions. As a result of this, the pH of treated water was increased. Furthermore, the values of pK_{a1} increased at higher concentration of Cl^- ions because more positively charged hydroxyl groups were generated on the MgOP surface. Consequently, the fluoride adsorption on MgOP was improved because of electrostatic attraction. In contrast, minor changes in the values of pK_{a1} were observed when $NaNO_3$ was served as the background electrolyte since NO_3^- ions negligibly affected the number of active adsorption sites on the MgOP surface and the fluoride adsorption on MgOP. In addition, the DLM was used to simulate the titration data and results showed the DLM could describe the titration process well ($R^2 > 0.99$).

3.2. Effect of initial pH on fluoride adsorption rate

MgOP (0.1 g) was added to test tubes containing 50 mL of fluoride solution (10 mg/L). The initial pH values of fluoride solution were adjusted to 3, 5, 7, 9 and 11 to evaluate the effects of initial pH values on fluoride adsorption rate (Fig. 3). Since the pseudo second-order kinetic model was proved to have high goodness-of-fit for the fluoride adsorption on MgOP

[15], the model was utilized to simulate the present process and its equation is described below:

$$\frac{t}{q_t} = \frac{1}{k_2 q_{em}^2} + \frac{t}{q_{em}} \quad (11)$$

where q_{em} is the equilibrated defluoridation capacity estimated by the pseudo second-order kinetic model; q_t (mg/g) is the defluoridation capacity at time t (min); and k_2 (g/mg·min) is the rate constant of the pseudo second-order kinetic model. From Table 3, results show that the model could well simulate the fluoride adsorption on MgOP (R^2 > 0.999). The adsorption rates (k_2) of fluoride at various initial pH values were present in this order: pH = 3 (0.3630 g/mg·min) > pH = 5 (0.1194 g/mg·min)> pH = 11 (0.1138 g/mg·min) > pH = 9 (0.0520 g/mg·min) > pH = 7 (0.0353 g/mg·min). Therefore, increasing concentration of H^+ or OH^- ions could increase the rate of fluoride adsorption on MgOP, most probably because of the hydroxyl groups on the surface of MgOP. As discussed in Section 3.1, positively and negatively charged hydroxyl groups could be generated on the MgOP surface under the acid and alkaline environments, respectively, while a neutral environment caused the formation of non-charged hydroxyl groups. Compared to the non-charged hydroxyl groups, the positively and negatively charged hydroxyl groups have higher affinity for fluoride adsorption. More importantly, the positively charged hydroxyl groups could more easily adsorb fluoride anions than the negatively charged hydroxyl groups due to electrostatic attraction. Notably, the pH values may not affect the total number of hydroxyl groups on the MgOP surface, so the equilibrated defluoridation capacity of MgOP was negligibly varied over a wide initial pH range (3 to 11).

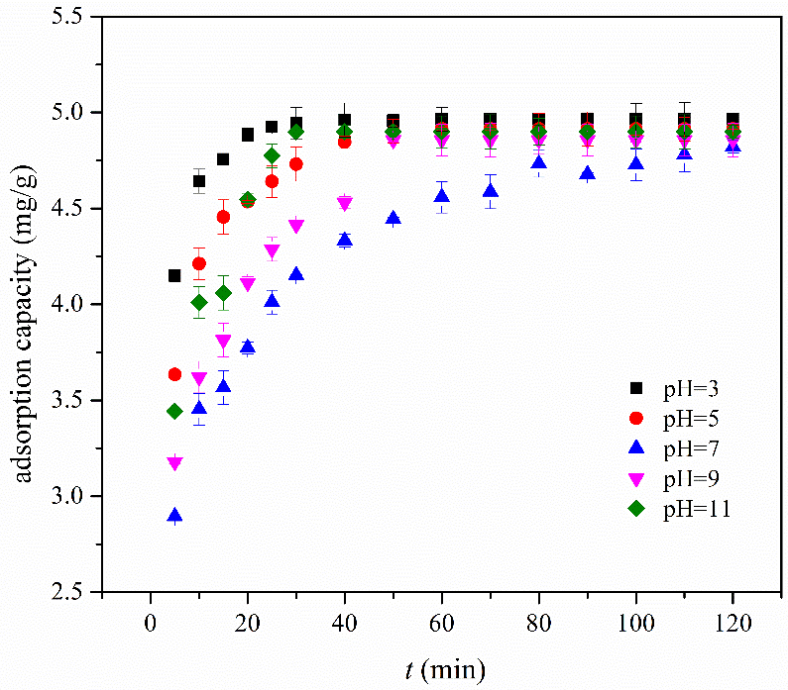

Fig. 3. Effects of initial pH on the adsorption rate of fluoride on MgOP (C_{MgOP} = 2 g/L, C_0 fluoride = 10 mg/L, temperature = 25 °C).

Table 3

Pseudo second-order kinetic model constants for the pH-dependent experiment

Adsorption model	Parameters	pH = 3	pH = 5	pH = 7	pH = 9	pH = 11
Experimental data[a]	q_e (mg/g)	4.964	4.914	4.822	4.856	4.899
pseudo second-order kinetics	q_{em} (mg/g)	4.995	5.003	5.008	5.051	4.998
	k_2 (g/mg·min)	0.3630	0.1194	0.0353	0.0520	0.1138
	R^2	1.000	0.9996	0.9995	0.9993	0.9996

[a] The experimental data represent the equilibrated defluoridation capacity (q_e).

3.3. Effect of aluminium salts on the fluoride adsorption

3.3.1. Effect of weight ratios of MgOP/aluminium salts

MgOP (0.1 g) and 50 mL of fluoride solution (30 mg/L) were mixed in the test tubes. To reveal the effects of aluminium salts on fluoride adsorption by MgOP, aluminum nitrate

310 ($Al[NO_3]_3$), aluminum chloride ($AlCl_3$) and aluminum sulfate ($Al_2[SO_4]_3$) were added to the
311 tubes at various weight ratios of MgOP to aluminum salts (1:1, 1:2, 1:3, 2:1 and 3:1). As
312 shown in Fig. 4, increasing quantity of aluminum salts facilitated the pH neutralization of
313 treated fluoride solutions, but slightly reduced the defluoridation capacity of MgOP.
314 Specifically, the equilibrated defluoridation capacities of MgOP were reduced from 14 mg/g
315 in the absence of aluminum salts to 10–13.5 mg/g in the presence of aluminum salts [15]. It
316 should be noted here that the addition of aluminum salts may cause the formation of $Al(OH)_3$
317 flocs/precipitates which can adsorb some of the fluoride ions. The discussion about the
318 fluoride adsorption in the presence of aluminum salts was conducted in Section 3.3.2.
319 Besides, using aluminum for the pH neutralization may not cause additional costs in the
320 wastewater treatment because aluminum salts are commonly employed as flocculants in the
321 process.

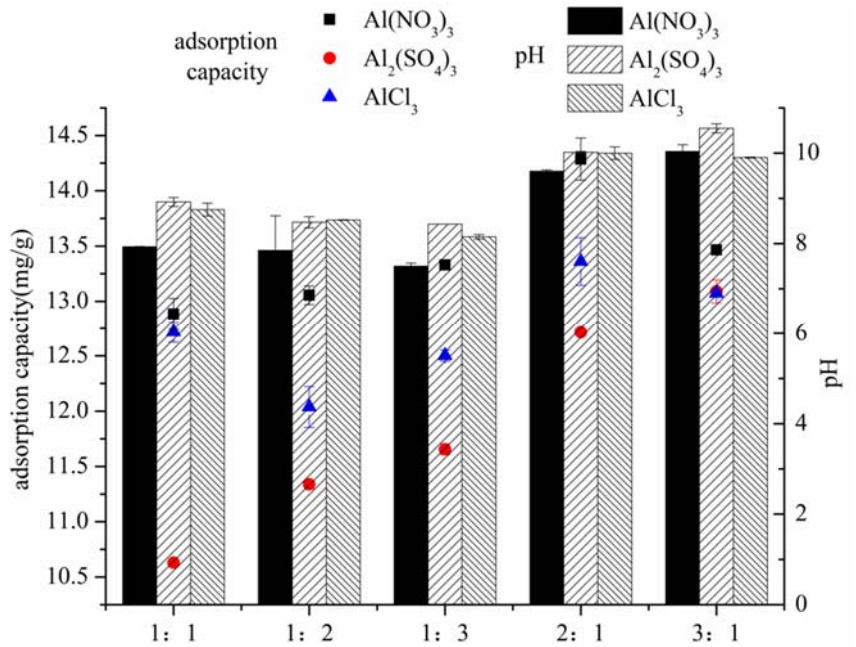

322

323 **Fig. 4.** Effect of aluminum salts on the fluoride adsorption of MgOP at different MgOP-to-
324 aluminum salts ratios (C_{MgOP} = 2 g/L, C_0 fluoride = 30 mg/L, temperature = 25 °C)**.**
325
326 The ability of aluminum salts to neutralize pH of treated fluoride solution followed the

order: $Al(NO_3)_3$ > $AlCl_3$ > $Al_2(SO_4)_3$. Based on WHO guidelines [4], the standard for NO_3^- ions in drinking water is stricter than that for SO_4^{2-} and Cl^-. Moreover, $AlCl_3$ is widely used as a flocculant in water treatment and the presence of Cl^- ions could improve the fluoride adsorption on MgOP as discussed in Section 3.1. Thus, $AlCl_3$ was preferred to be used to neutralize pH of treated fluoride solution in this study. When the weight ratios of MgOP to $AlCl_3$ were 1:1 and 1:3, the equilibrated defluoridation capacities of MgOP were 12.1 and 12.7 mg/g, respectively, while the corresponding pH values of treated solution were 8.15 and 8.75. Therefore, an increased MgOP:$AlCl_3$ weight ratio may not significantly affect the equilibrated defluoridation capacity of MgOP and pH neutralization of treated fluoride solution. For this reason, the MgOP:$AlCl_3$ weight ratio of 1:1 was utilized in subsequent experiments.

Furthermore, > 0.2 mg/L of Al^{3+} ions in drinking water may detrimentally influence the human health, so the concentrations of Al^{3+} in treated water were tested at the MgOP:$AlCl_3$ weight ratio of 1:1, initial fluoride solution of 10-30 mg/L and reaction time of 90 min. Results suggested the concentrations of Al^{3+} in treated water were less than 0.2 mg/L, which indicated that it is safe to use $AlCl_3$ for the pH neutralization of treated water at such ratio.

3.3.2. Effect of contact time

To further understand the effects of $AlCl_3$ on fluoride adsorption, the fluoride adsorption on MgOP in the presence of $AlCl_3$ was examined as a function of contact time (5, 10, 15, 20, 25, 30, 40, 50, 60, 70, 80 and 90 min). Test tubes containing 0.1 g each of MgOP and $AlCl_3$ and 50 mL of fluoride solution with different initial fluoride concentrations (10, 15, 20 and 25 mg/L) were shaken, which was then used to measure remaining fluoride concentration and pH of treated water.

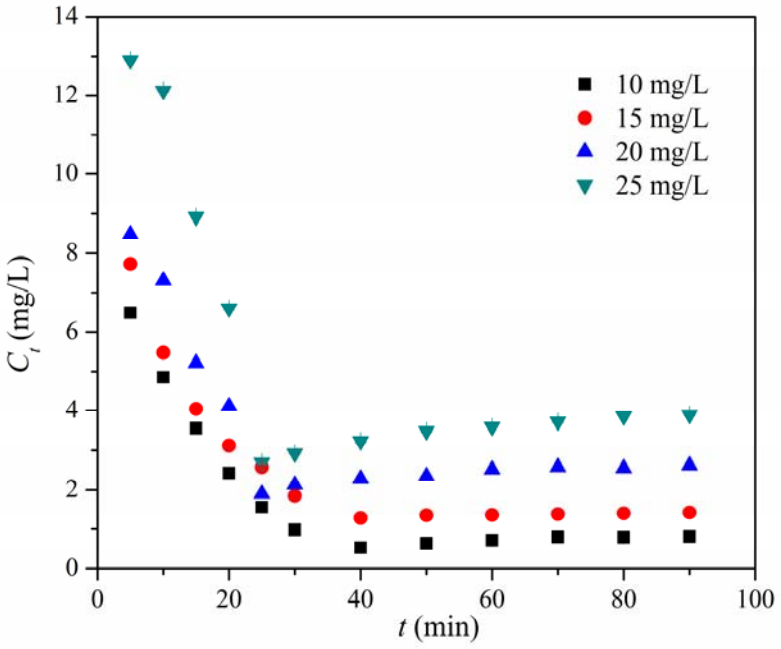

Fig. 5. Fluoride adsorption on MgOP in the presence of $AlCl_3$ as a function of time and initial fluoride concentration (C_{MgOP} = 2 g/L, temperature = 25 °C, pH = 7.0, "C_t" represents the concentrations of fluoride ions in solution).

The kinetic curves (Fig. 5) for initial fluoride concentrations of 10, 15, 20 and 25 mg/L had similar trends. It is logical for the fluoride concentrations of treated water to have the minimum value at equilibrium. However, the minimum concentration of fluoride was observed before equilibrium, which was attributed to the complexation and dissociation between Al^{3+} and F^- ions. In the aquatic environment, when fluoride and aluminum ions come in contact, aluminum ions can avidly bind with fluoride ions to form an aluminofluoride complex (AlF_x) as described by the Equations (12) and (13) [31, 32]. The chemical interaction between Al^{3+} and F^- can only occur in an acidic environment because alkaline pH may lead to dissociate AlF_x.

$$\equiv AlOH + H^+ \leftrightarrow AlOH_2^+$$

$$\equiv AlOH_2^+ + F^- \leftrightarrow AlF + H_2O$$

$$\equiv AlOH + F^- \leftrightarrow AlF + OH^- \quad (12)$$

Simultaneously, the dissociative aluminum ions can also react with fluoride ions as shown below:

$$Al^{3+} + F^{-} \leftrightarrow AlF^{2+}$$

$$Al^{3+} + 2F^{-} \leftrightarrow AlF_2^{+}$$

$$Al^{3+} + 3F^{-} \leftrightarrow AlF_3$$

$$Al^{3+} + 4F^{-} \leftrightarrow AlF_4^{-}$$

$$Al^{3+} + 5F^{-} \leftrightarrow AlF_5^{2-}$$

$$Al^{3+} + 6F^{-} \leftrightarrow AlF_6^{3-} \quad (13)$$

With the help of Visual MINTEQ 3.1 software, the possible reactions between Al^{3+} and F^- ions in the present research are presented in Fig. 6.

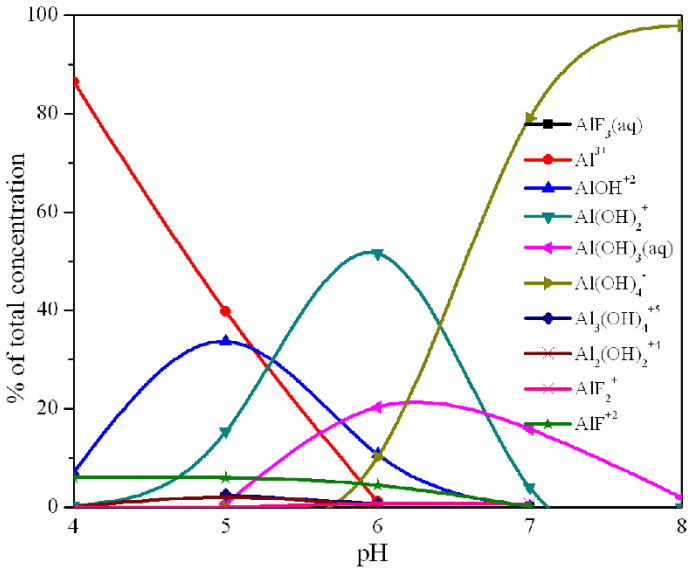

Fig. 6. Forms of aluminum ions in the fluoride adsorption process at pH range 4–8.

In the beginning, some fluoride ions reacted with Al^{3+} ions to form AlF_x (Fig. 6). However, the ability of Al^{3+} ions to bind fluoride ions gradually became weakened at pH > 6. As a result of this, fluoride ions bound with Al^{3+} ions may release from AlF_x to the solution,

increasing the fluoride concentrations. Simultaneously, the adsorption ability of $Al(OH)_3$ flocs/precipitates for may also lose efficacy at pH > 6. Hence, pH = 6 was the critical point for the fluoride adoption in the presence of Al^{3+}. The effects of contact time on pH of treated fluoride solution were investigated (Fig. S2) and results showed that the pH reached 6 at 40 min at the initial fluoride concentrations of 10 and 15 mg/L, which was also the time that the minimum value of remaining fluoride concentration occurred (Fig. 5). Similar patterns were also observed at 25 min when the initial fluoride concentrations were 20 and 25 mg/L.

4. Conclusions

Results from this research justify the following main conclusions.

(1) MgOP can more easily adsorb H^+ ions than OH^- ions, which result in the pH elevation of treated fluoride solution. Furthermore, the presence of Cl^- improves fluoride adsorption on the MgOP while fluoride adsorption is insignificantly affected by $NaNO_3$ as the background electrolyte.

(2) The adsorption of H^+ and OH^- ions on MgOP can only influence the electrical charges of hydroxyl groups on the MgOP surface, but not the total amount of these groups. Consequently, the equilibrated defluoridation capacity of MgOP is independent on pH.

(3) $AlCl_3$ could effectively neutralize the pH of treated fluoride solution. The reaction between Al^{3+} and F^- ions may decrease the equilibrated defluoridation capacity of MgOP to a value that is slightly less than its maximum value.

Acknowledgment

This work was financially supported by the National Natural Science Foundation of China (51409108) and National Natural Science Foundation of China (21177045).

References

[1] A.D. Atasoy, M.O. Sahin, Adsorption of fluoride on the raw and modified cement clay, CLEAN-Soil, Air, Water 42 (2014) 415-420.

[2] L.H. Velazquez-Jimenez, R.H. Hurt, J. Matos, J.R. Rangel-Mendez, Zirconium-carbon hybrid sorbent for removal of fluoride from water: oxalic acid mediated Zr(IV) assembly and adsorption mechanism, Environ. Sci. Technol. 48 (2013) 1166-1174.

[3] S.V. Jadhav, E. Bringas, G.D. Yadav, V.K. Rathod, I. Ortiz, K.V. Marathe, Arsenic and fluoride contaminated groundwaters: a review of current technologies for contaminants removal, J. Environ. Manage. 162 (2015) 306-325.

[4] WHO, Guidelines for drinking-water quality, Geneva: world health organization 2011.

[5] A. Bretzler, C.A. Johnson, The Geogenic Contamination Handbook: Addressing arsenic and fluoride in drinking water, Appl. Geochem. 63 (2015) 642-646.

[6] H. Amini, G.A. Haghighat, M. Yunesian, R. Nabizadeh, A.H. Mahvi, M.H. Dehghani, R. Davani, A.-R. Aminian, M. Shamsipour, N. Hassanzadeh, Spatial and temporal variability of fluoride concentrations in groundwater resources of Larestan and Gerash regions in Iran from 2003 to 2010, Environ. Geochem. Health 38 (2016) 25-37.

[7] M. Shams, R. Nabizadeh Nodehi, M. Hadi Dehghani, M. Younesian, A. Hossein Mahvia, Efficiency of granular ferric hydroxide (GFH) for removal of fluoride from water, Fluoride 43 (2010) 61.

[8] M.H. Dehghani, M. Faraji, A. Mohammadi, H. Kamani, Optimization of fluoride adsorption onto natural and modified pumice using response surface methodology: Isotherm, kinetic and thermodynamic studies, Korean J. Chem. Eng. 34 (2017) 454-462.

[9] L.-X. Li, D. Xu, X.-Q. Li, W.-C. Liu, Y. Jia, Excellent fluoride removal properties of porous hollow MgO microspheres, New J. Chem. 38 (2014) 5445-5452.

[10] T. Suzuki, A. Nakamura, M. Niinae, H. Nakata, H. Fujii, Y. Tasaka, Immobilization of

fluoride in artificially contaminated kaolinite by the addition of commercial-grade magnesium oxide, Chem. Eng. J. 233 (2013) 176-184.

[11] D.Q. Zhou, M. He, Y.H. Zhang, M.Y. Huang, Y.Y. Jiang, Asymmetric hydrogenation of diketones catalyzed by magnesium oxide-supported chitosan-Rh complex, Polym. Adv. Technol. 14 (2003) 287-291.

[12] Z. Jin, Y. Jia, K.-S. Zhang, L.-T. Kong, B. Sun, W. Shen, F.-L. Meng, J.-H. Liu, Effective removal of fluoride by porous MgO nanoplates and its adsorption mechanism, J. Alloys Compd. 675 (2016) 292-300.

[13] S.G. Lee, J.-W. Ha, E.-H. Sohn, I.J. Park, S.-B. Lee, Synthesis of pillar and microsphere-like magnesium oxide particles and their fluoride adsorption performance in aqueous solutions, Korean J. Chem. Eng. 34 (2017) 2738-2747.

[14] T. Kameda, Y. Yamamoto, S. Kumagai, T. Yoshioka, Analysis of F^- removal from aqueous solutions using MgO, J. Water Proc. Eng. 25 (2018) 54-57.

[15] J. Kang, B. Li, J. Song, D. Li, J. Yang, W. Zhan, D. Liu, Defluoridation of water using calcined magnesia/pullulan composite, Chem. Eng. J. 166 (2011) 765-771.

[16] M. Nazari, R. Halladj, Adsorptive removal of fluoride ions from aqueous solution by using sonochemically synthesized nanomagnesia/alumina adsorbents: An experimental and modeling study, J. Taiwan. Inst. Chem. E 45 (2014) 2518-2525.

[17] H. Deng, Y. Chen, Y. Cao, W. Chen, Enhanced phosphate and fluoride removal from aqueous solution by ferric-modified chromium (Ⅲ)-fibrous protein, J. Taiwan. Inst. Chem. E 68 (2016) 323-331.

[18] S. Manna, D. Roy, P. Saha, B. Adhikari, Defluoridation of aqueous solution using alkali–steam treated water hyacinth and elephant grass, J. Taiwan. Inst. Chem. E 50 (2015) 215-222.

[19] Y. Ye, J. Yang, W. Jiang, J. Kang, Y. Hu, H.H. Ngo, W. Guo, Y. Liu, Fluoride removal from water using a magnesia-pullulan composite in a continuous fixed-bed column, J.

459 Environ. Manage. 206 (2018) 929-937.
460 [20] M. Vithanage, A.U. Rajapaksha, M. Bootharaju, T. Pradeep, Surface complexation of
461 fluoride at the activated nano-gibbsite water interface, Colloids Surf. Physicochem. Eng.
462 Aspects 462 (2014) 124-130.
463 [21] Z. He, R. Liu, J. Xu, H. Liu, J. Qu, Defluoridation by Al-based coagulation and
464 adsorption: species transformation of aluminum and fluoride, Sep. Purif. Technol. 148 (2015)
465 68-75.
466 [22] S. Padhi, T. Tokunaga, Surface complexation modeling of fluoride sorption onto calcite,
467 J. Environ. Chem. Eng. 3 (2015) 1892-1900.
468 [23] R. Weerasooriya, H. Wickramarathne, H. Dharmagunawardhane, Surface complexation
469 modeling of fluoride adsorption onto kaolinite, Colloids Surf. Physicochem. Eng. Aspects
470 144 (1998) 267-273.
471 [24] D. Langmuir, Aqueous environmental geochemistry, Prentice–Hall, Englewood Cliffs,
472 NJ1997.
473 [25] C.K. Na, H.J. Park, Defluoridation from aqueous solution by lanthanum hydroxide, J.
474 Hazard. Mater. 183 (2010) 512–520.
475 [26] H.A. Al-Hosney, V.H. Grassian, Carbonic acid: An important intermediate in the surface
476 chemistry of calcium carbonate, J. Am. Chem. Soc. 126 (2004) 8068-8069.
477 [27] Q. Du, Z. Sun, W. Forsling, H. Tang, Acid-base properties of aqueous illite surfaces, J.
478 Colloid Interface Sci. 187 (1997) 221-231.
479 [28] C. Chen, J. Hu, D. Xu, X. Tan, Y. Meng, X. Wang, Surface complexation modeling of Sr
480 (II) and Eu (III) adsorption onto oxidized multiwall carbon nanotubes, J. Colloid Interface
481 Sci. 323 (2008) 33-41.
482 [29] P. Zhou, H. Yan, B. Gu, Competitive complexation of metal ions with humic substances,
483 Chemosphere 58 (2005) 1327-1337.

[30] D.A. Dzombak, F.M. Morel, Surface complexation modeling: hydrous ferric oxide, John Wiley & Sons1990.

[31] A. Strunecka, R.L. Blaylock, O. Strunecky, Fluoride, aluminum, and aluminofluoride complexes in pathogenesis of the autism spectrum disorders: A possible role of immunoexcitotoxicity, J. Appl. Biomed. 14 (2016) 171-176.

[32] Y. Wang, E.J. Reardon, Activation and regeneration of a soil sorbent for defluoridation of drinking water, Appl. Geochem. 16 (2001) 531-539.